www.ietdl.org

Published in IET Microwaves, Antennas & Propagation
Received on 22nd September 2012
Revised on 25th February 2013
Accepted on 18th March 2013
doi: 10.1049/iet-map.2012.0553

ISSN 1751-8725

Technique for inversion of an inhomogeneous bianisotropic slab through an optimisation approach

Ali Farahbakhsh, Davoud Zarifi, Ali Abdolali, Mohammad Soleimani

Department of Electrical Engineering, Iran University of Science and Technology, Tehran, Iran
E-mail: a_farahbakhsh@iust.ac.ir

Abstract: An electromagnetic inversion method is presented to reconstruct the constitutive parameters of an inhomogeneous bianisotropic slab. The measured co- and cross-reflection and transmission coefficients are used to extract the electromagnetic parameters profiles of the inhomogeneous bianisotropic media from the proposed method, using truncated Fourier series expansion and Gravitational Search Algorithm (GSA). GSA is used to improve the speed and accuracy of the optimisation process because of the complexity of inhomogeneous bianisotropic media, highly non-linearity of optimisation problem, and extremely large search space. Finally, the accuracy and robustness of the proposed reconstruction method are validated using some typical examples.

1 Introduction

Features of electromagnetic wave propagation in bianisotropic media have been intensively studied during the last few decades. Owing to the need for special electromagnetic properties, complex materials, such as bianisotropic media, classified as materials exhibiting magnetoelectric coupling, are considered. In these materials, there is a coupling between electric and magnetic fields which causes simultaneous production of electric and magnetic polarisations because of the electric or magnetic excitation [1]. This phenomenon is mathematically represented by magnetoelectric coupling tensors in constitutive relations. Bianisotropic media incorporates large variety of media, such as chiral or bi-isotropic media, gyrotropic chiral media, Faraday chiral media, anisotropic media, and gyrotropic media. Various applications utilising bianisotropic media have been proposed such as antenna radome [2], waveguides [3, 4] and polarisation transformers [5], microstrip antennas [6, 7], absorbers [8], backward wave media [9], and cloaking materials [10].

Electromagnetic scattering is one of the basic problems in the study of interaction of electromagnetic waves with bianisotropic media. If the structures of complex media are not in canonical geometries, the analytical analysis is limited. In this connection, many numerical methods have been extended to study the interaction of electromagnetic wave with complex media such as finite difference time domain [11, 12], and finite element method [13].

Analysis of the wave propagation and scattering from planar layered homogeneous bianisotropic mediums is rather straightforward. Rikte *et al.* introduced an efficient and robust method namely notation of propagators and wave splitting approach for analysing scattering from planar layered homogeneous bianisotropic media [14].

The problem of wave propagation in inhomogeneous media is important in many practical situations. Exact solution of the wave equation in such media is known for only a few particular profiles; and because of this, the wave propagation and scattering from inhomogeneous media has been intensively investigated and several approaches have been presented [15–22]. Recently, notation of propagator and wave splitting method is extended to analysis of inhomogeneous planar layered bianisotropic media [23]. An optimisation-based technique has been presented in [24] to simultaneously evaluate the permeability, permittivity and chirality parameter of a homogeneous bianisotropic slab from the knowledge of the transmission and reflection coefficients. In the present paper, a robust method is presented to reconstruct the constitutive parameters of an inhomogeneous bianisotropic slab via an advanced optimisation approach entitled Gravitational Search Algorithm (GSA).

The paper is organised as follows: The analysis of forward problem is reviewed in Section 2. In Section 3, applicability of the optimisation approach to reconstruct of inhomogeneous bianisotropic slab electromagnetic parameters is investigated. Section 4 is devoted to the verification of the accuracy of the proposed method. Finally, summary and conclusions are provided in Section 5.

2 Forward problem analysis

Electromagnetic inversion is achieved by solving out for the profiles which minimises the error between the observed data and the synthetic one which is obtained by analysing the forward problem. In this section, the forward problem is reviewed first.

Consider a reciprocal inhomogeneous bianisotropic slab characterised by constitutive relations [1]

$$\begin{bmatrix} \overline{D} \\ \overline{B} \end{bmatrix} = \begin{bmatrix} \overline{\overline{\varepsilon}}(z) & \mathrm{j}\sqrt{\mu_0\varepsilon_0}\overline{\overline{\kappa}}(z) \\ -\mathrm{j}\sqrt{\mu_0\varepsilon_0}\overline{\overline{\kappa}}^{\mathrm{T}}(z) & \overline{\overline{\mu}}(z) \end{bmatrix} \begin{bmatrix} \overline{E} \\ \overline{H} \end{bmatrix} \quad (1)$$

where $\overline{D}$, $\overline{B}$, $\overline{E}$ and $\overline{H}$ are the electromagnetic field vectors, and $\bar{\bar{\varepsilon}}$, $\bar{\bar{\mu}}$, and $\bar{\bar{\kappa}}$, represent the medium permittivity, permeability and magneto-electric or chirality parameter tensors, respectively. The superscript T stands for transpose, and two conditions $\bar{\bar{\varepsilon}} = \bar{\bar{\varepsilon}}^{\mathrm{T}}$ and $\bar{\bar{\mu}} = \bar{\bar{\mu}}^{\mathrm{T}}$ are the familiar requirements on the symmetry of permittivity and permeability tensors. As shown in Fig. 1, both sides of the inhomogeneous bianisotropic slab having thickness d are free space and a plane wave impinges with an angle θ_i from free space onto it. In the forward problem, the reflection and transmission coefficients of inhomogeneous bianisotropic slab are calculated by the notation of propagators technique for inhomogeneous media which has been described in [23]. Using the Maxwell's equations and assuming $\exp(-\mathrm{j}\omega t)$ time conversion, the tangential components of the electric and magnetic fields, that is $\overline{E}_{xy}$ and $\overline{H}_{xy}$, satisfy the following equations

$$\frac{\mathrm{d}}{\mathrm{d}z}\begin{bmatrix} \overline{E}_{xy}(z) \\ \eta_0\overline{\overline{J}}\,\overline{H}_{xy}(z) \end{bmatrix} = \mathrm{j}k_0\overline{\overline{M}}(z)\begin{bmatrix} \overline{E}_{xy}(z) \\ \eta_0\overline{\overline{J}}.\overline{H}_{xy}(z) \end{bmatrix} \quad (2)$$

where k_0 is the wave number in the free space, η_0 is the free-space intrinsic impedance, $\bar{\bar{J}}$ is two-dimensional rotation dyadic, and $\bar{\bar{M}}$ is the fundamental dyadic of the inhomogeneous bianisotropic medium whose elements depend on the tangential wave vector and the constitutive tensors of the medium can be found in [14, 23]. At the boundary $z = d$ we can write

$$\begin{bmatrix} \overline{E}_{xy}(d) \\ \eta_0\overline{\overline{J}}\,\overline{H}_{xy}(d) \end{bmatrix} = \bar{\bar{P}}\begin{bmatrix} \overline{E}_{xy}(z=0) \\ \eta_0\overline{\overline{J}}.\overline{H}_{xy}(z=0) \end{bmatrix} \quad (3)$$

where $\bar{\bar{P}} = \mathrm{e}^{\mathrm{j}k_0 d\bar{\bar{M}}}$ is the propagator dyadic. In the case of inhomogeneous media, the layer can be decomposed into thin homogeneous sub-layers and the propagator dyadic of the layer is determined by multiplication of the propagator dyadics of its sub-layers. The transverse reflection and transmission dyadics $\bar{\bar{r}}_{xy}$ and $\bar{\bar{t}}_{xy}$, whose multiplications by the transverse incident field reveal the transverse reflected and transmitted fields, are defined by

$$\begin{cases} \overline{E}^r_{xy}(0) = \bar{\bar{r}}_{xy}\overline{E}^i_{xy}(0) \\ \overline{E}^t_{xy}(d) = \bar{\bar{t}}_{xy}\overline{E}^i_{xy}(0) \end{cases} \quad (4)$$

where i, r, and t subscripts indicate the incident, reflected, and transmitted waves, respectively. It can be seen that the reflection and transmission dyads for the tangential electric field are determined by

$$\begin{cases} \bar{\bar{r}}_{xy} = -\overline{\overline{T}}_{22}^{-1}\overline{\overline{T}}_{21} \\ \bar{\bar{t}}_{xy} = \overline{\overline{T}}_{11} + \overline{\overline{T}}_{12}\bar{\bar{r}}_{xy} \end{cases} \quad (5)$$

wherein

$$\begin{bmatrix} \overline{\overline{T}}_{11} & \overline{\overline{T}}_{12} \\ \overline{\overline{T}}_{21} & \overline{\overline{T}}_{22} \end{bmatrix} = \frac{1}{2}\begin{bmatrix} \bar{\bar{I}}_t & -\overline{\overline{O}} \\ \bar{\bar{I}}_t & \overline{\overline{O}} \end{bmatrix}\begin{bmatrix} \overline{\overline{P}}_{11} & \overline{\overline{P}}_{12} \\ \overline{\overline{P}}_{21} & \overline{\overline{P}}_{22} \end{bmatrix} \times \begin{bmatrix} \bar{\bar{I}}_t & \bar{\bar{I}}_t \\ -\overline{\overline{O}}^{-1} & \overline{\overline{O}}^{-1} \end{bmatrix} \quad (6)$$

where $\bar{\bar{I}}_t = \hat{a}_x\hat{a}_x + \hat{a}_y\hat{a}_y$ is the two-dimensional identity dyadic, $\overline{\overline{O}}^{-1} = k_0/k_z\left[\bar{\bar{I}}_t + 1/k_0^2\,\bar{k}_t \times \left(\bar{k}_t \times \bar{\bar{I}}_t\right)\right]$, and $\bar{k}_t$ and k_z are the tangential and normal components of the incident and reflected wave vectors, respectively.

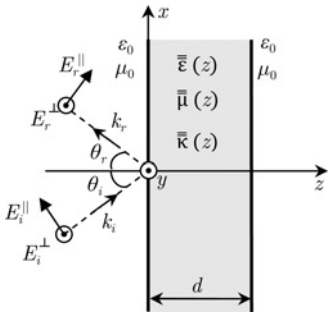

Fig. 1 *Inhomogeneous bianisotropic slab exposed to an incident plane wave with TM* $\left(E_i^{\parallel}\right)$ *or TE* $\left(E_i^{\perp}\right)$ *polarisations*

3 Optimisation approach to inverse problem

In the inverse problem, it is tried to match the data calculated from the forward problem, that is co- and cross-reflection and transmission coefficients, with the data obtained from the measurement; so that the constitutive parameters of medium supporting this match are considered as the solution of the inverse problem.

In reconstructing the inhomogeneous slab, it is recommended to use any suitable expansion function for the continuous profile models. Expansion functions such as the linear, cosine and Legendre forms can be used. However, it is recommended to use the model which can perform the profile reconstruction with minimum number of terms. Through the inversion process, it is found that the cosine expansion model has better performance for the many of profiles rather than other expansion functions. Here, the functions of permittivity, permeability and magneto-electric tensors of inhomogeneous bianisotropic layer, are

considered as the following Fourier series expansions (see (7–9))

The problem is to find the coefficients of Fourier expansions of constitutive parameters. This is usually done through the utilisation of an optimisation method that minimises the error between the measured and calculated data. Considering N terms in each Fourier series expansion yields an extremely large search space with $21(N+1)$ dimensions. Obtaining the optimal solution in this search space by ordinary methods is infinitely difficult and time consuming. In fact, local optimisation methods such as quasi-Newton and Gauss-Newton techniques [25, 26] are relatively fast but have the possibility of being trapped in local minima because of the severely non-linear nature of the problem. On the other hand, convergence of global optimisation techniques such as genetic algorithm [27] and particle swarm [28] is reached after very large number of iterations. Therefore here, an advanced and robust optimisation technique entitled the GSA is utilised [29]. We define the objective function as

$$F = \sum_{\mathrm{TE,TM}} \sum_{\theta=\theta_s}^{\theta e} \left[\left| \tilde{R}_{\mathrm{co}}(\theta) - R^m_{\mathrm{co}}(\theta) \right| + \left| \tilde{T}_{\mathrm{co}}(\theta) - T^m_{\mathrm{co}}(\theta) \right| + \left| \tilde{R}_{\mathrm{cr}}(\theta) - R^m_{\mathrm{cr}}(\theta) \right| + \left| \tilde{T}_{\mathrm{cr}}(\theta) - T^m_{\mathrm{cr}}(\theta) \right| \right] \tag{10}$$

where $\tilde{R}(\theta)$ and $\tilde{T}(\theta)$ are the calculated reflection and transmission coefficients, respectively, and $R^m(\theta)$ and $T^m(\theta)$ are the measured ones. Also, the indices 'co' and 'cr' represent the co- and cross-polarised coefficients, and θ_s and θ_e are the limits of incident angle. The optimisation method seeks at minimising the objective function, which is obtained when the measured and calculated transmission and reflection coefficients are identical, indicating that the reconstructed constitutive parameters are identical to the original ones.

In GSA, agents are assumed to be objects and their masses are considered as their performance. The gravity force causes attraction between these objects, and all objects are moved towards the objects with heavier masses by the gravity force and also the heavier objects move slower than lighter ones. The good solutions are shown by the heavy object. In GSA, each mass presents a solution, and the algorithm is navigated by properly adjusting the masses. By lapse of time, it is expected that masses to be attracted by the heaviest mass. The heaviest mass will present an optimum solution in the search space.

One of the advantages of the GSA is its ability to find optimum solution in a large search space. However, our search space is extremely large and the GSA cannot work properly in this space. To overcome this dilemma, a multi-search GSA is used. In this method, the GSA is run to explore the whole search space and obtain primary results. Next, the search space is limited to find only the first Nth unknown coefficients, that is $E_{11,n}$, whereas the other unknown coefficients is assumed to be the primary results. This process is done for the other elements of constitutive tensors. The whole method is repeated twice or more until the best solution is found.

The importance of the thickness of the slab in the optimisation process should be carefully regarded. In fact, if the slab is very thin compared with the wavelength, it is almost transparent so that the reflection coefficients are almost zero and the transmissions ones are almost unity. On the other hand, if the slab is very thick, the problem becomes extremely non-linear and is more difficult to optimise.

4 Numerical examples and results

For the purpose of illustration, the applicability and robustness of the proposed inversion method are applied to

$$\bar{\bar{\varepsilon}}(z) = \varepsilon_0 \begin{bmatrix} \varepsilon_{11}(z) & \varepsilon_{12}(z) & \varepsilon_{13}(z) \\ \varepsilon_{21}(z) & \varepsilon_{22}(z) & \varepsilon_{23}(z) \\ \varepsilon_{31}(z) & \varepsilon_{32}(z) & \varepsilon_{33}(z) \end{bmatrix} = \varepsilon_0 \begin{bmatrix} \sum_{n=0}^{N} E_{11,n} \cos\left(\frac{n\pi z}{d}\right) & \sum_{n=0}^{N} E_{12,n} \cos\left(\frac{n\pi z}{d}\right) & \sum_{n=0}^{N} E_{13,n} \cos\left(\frac{n\pi z}{d}\right) \\ \sum_{n=0}^{N} E_{21,n} \cos\left(\frac{n\pi z}{d}\right) & \sum_{n=0}^{N} E_{22,n} \cos\left(\frac{n\pi z}{d}\right) & \sum_{n=0}^{N} E_{23,n} \cos\left(\frac{n\pi z}{d}\right) \\ \sum_{n=0}^{N} E_{31,n} \cos\left(\frac{n\pi z}{d}\right) & \sum_{n=0}^{N} E_{32,n} \cos\left(\frac{n\pi z}{d}\right) & \sum_{n=0}^{N} E_{33,n} \cos\left(\frac{n\pi z}{d}\right) \end{bmatrix} \tag{7}$$

$$\bar{\bar{\mu}}(z) = \mu_0 \begin{bmatrix} \mu_{11}(z) & \mu_{12}(z) & \mu_{13}(z) \\ \mu_{21}(z) & \mu_{22}(z) & \mu_{23}(z) \\ \mu_{31}(z) & \mu_{32}(z) & \mu_{33}(z) \end{bmatrix} = \mu_0 \begin{bmatrix} \sum_{n=0}^{N} M_{11,n} \cos\left(\frac{n\pi z}{d}\right) & \sum_{n=0}^{N} M_{12,n} \cos\left(\frac{n\pi z}{d}\right) & \sum_{n=0}^{N} M_{13,n} \cos\left(\frac{n\pi z}{d}\right) \\ \sum_{n=0}^{N} M_{21,n} \cos\left(\frac{n\pi z}{d}\right) & \sum_{n=0}^{N} M_{22,n} \cos\left(\frac{n\pi z}{d}\right) & \sum_{n=0}^{N} M_{23,n} \cos\left(\frac{n\pi z}{d}\right) \\ \sum_{n=0}^{N} M_{31,n} \cos\left(\frac{n\pi z}{d}\right) & \sum_{n=0}^{N} M_{32,n} \cos\left(\frac{n\pi z}{d}\right) & \sum_{n=0}^{N} M_{33,n} \cos\left(\frac{n\pi z}{d}\right) \end{bmatrix} \tag{8}$$

$$\bar{\bar{\kappa}}(z) = \begin{bmatrix} \kappa_{11}(z) & \kappa_{12}(z) & \kappa_{13}(z) \\ \kappa_{21}(z) & \kappa_{22}(z) & \kappa_{23}(z) \\ \kappa_{31}(z) & \kappa_{32}(z) & \kappa_{33}(z) \end{bmatrix} = \begin{bmatrix} \sum_{n=0}^{N} K_{11,n} \cos\left(\frac{n\pi z}{d}\right) & \sum_{n=0}^{N} K_{12,n} \cos\left(\frac{n\pi z}{d}\right) & \sum_{n=0}^{N} K_{13,n} \cos\left(\frac{n\pi z}{d}\right) \\ \sum_{n=0}^{N} K_{21,n} \cos\left(\frac{n\pi z}{d}\right) & \sum_{n=0}^{N} K_{22,n} \cos\left(\frac{n\pi z}{d}\right) & \sum_{n=0}^{N} K_{23,n} \cos\left(\frac{n\pi z}{d}\right) \\ \sum_{n=0}^{N} K_{31,n} \cos\left(\frac{n\pi z}{d}\right) & \sum_{n=0}^{N} K_{32,n} \cos\left(\frac{n\pi z}{d}\right) & \sum_{n=0}^{N} K_{33,n} \cos\left(\frac{n\pi z}{d}\right) \end{bmatrix} \tag{9}$$

doi: 10.1049/iet-map.2012.0553

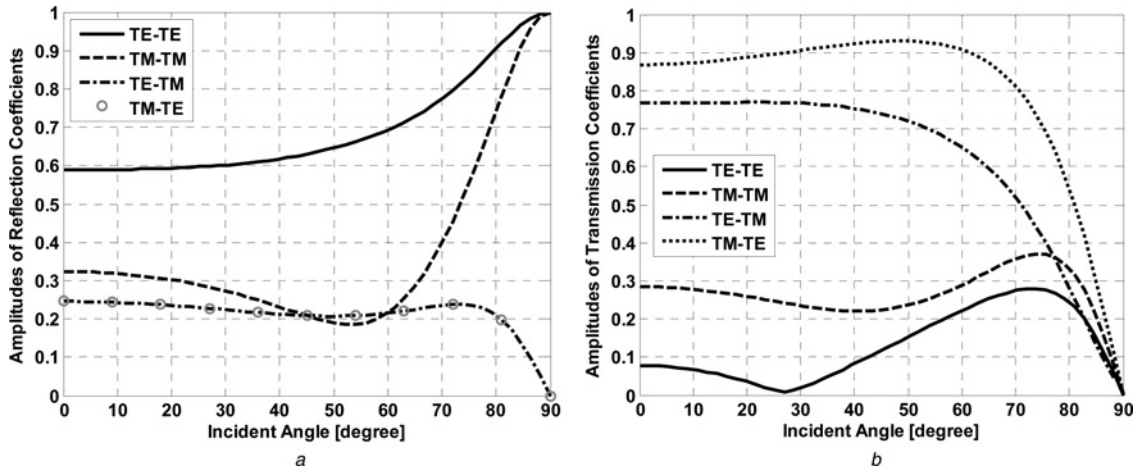

Fig. 2 *Amplitudes of co- and cross-reflection and transmission coefficients as a function of incident angle θ_i for inhomogeneous bianisotropic slab*

a Reflection slab discussed in example 1
b Transmission

three different typical models. The illustrated models are inhomogeneous bianisotropic slabs, either embedded in a free space, or backed by a perfect electric conductor (PEC) plane. In these numerical examples, the co- and cross-reflection and transmission coefficients are first calculated using the forward problem solver, and then they are used to evaluate the optimised parameters in the inverse process.

4.1 Example 1

As the first example, consider an inhomogeneous bianisotropic slab with thickness of $d = 5$ cm, and the typical profiles of the relative permittivity, relative permeability, and chirality parameter tensors as follows

$$\bar{\bar{\varepsilon}}(z) = \varepsilon_0 \begin{pmatrix} \exp\left(\frac{z}{2d}\right) & \frac{3}{1+\frac{z}{d}} & 0 \\ \frac{3}{1+\frac{z}{d}} & 1+\frac{z}{d} & 0 \\ 0 & 0 & 2+\cos\left(\frac{\pi z}{d}\right) \end{pmatrix} \tag{11}$$

$$\bar{\bar{\mu}}(z) = \mu_0 \bar{\bar{I}}_{(3\times 3)} \tag{12}$$

$$\bar{\bar{\kappa}}(z) = \begin{pmatrix} \exp\left(\frac{z}{d}\right) & 0 & 0 \\ 0 & \exp\left(\frac{z}{2d}\right) & 0 \\ 0 & 0 & \exp\left(\frac{z}{3d}\right) \end{pmatrix} \tag{13}$$

which is embedded in free space. The amplitudes of co- and cross-reflection and transmission coefficients against the angle of incidence at excitation frequency of 1 GHz obtained from the forward problem solver are shown in Fig. 2.

In the inverse problem, assuming $N = 7$ terms for each Fourier series expansion in (7–9), the proposed inversion algorithm is applied to the transmission and reflection data. Using GSA algorithm, the unknown coefficients of Fourier series expansions are optimised so that the calculated co- and cross-reflection and transmission data match the measured ones. These evaluated coefficients are written in Table 1. The final reconstructed profiles of relative permittivity and chirality parameter tensors are shown in Figs. 3*a* and *b*. From these figures, observe that the accuracy of the inversion is quite satisfactory.

4.2 Example 2

The general procedure in this example starts with the assumption that the electromagnetic parameters of a given

Table 1 Optimisation results for the truncated Fourier series expansions of electromagnetic parameters of inhomogeneous bianisotropic slab in free space (example 1)

Coefficients	$n=0$	$n=1$	$n=2$	$n=3$	$n=4$	$n=5$	$n=6$	$n=7$
$E_{11,n}$	1.2975	−0.2609	0.0162	−0.0287	0.0036	−0.0093	0.0012	−0.0034
$E_{12,n}$	2.0792	0.5749	0.0975	0.0777	0.0256	0.0261	0.0087	0.0087
$E_{22,n}$	1.5000	−0.4044	0.0000	−0.0433	0.0000	−0.0139	0.0000	−0.0047
$E_{33,n}$	2.0000	1.0000	0.0000	0.0000	0.0000	0.0000	0.0000	0.0000
other $E_{ij,n}$	0.0000	0.0000	0.0000	0.0000	0.0000	0.0000	0.0000	0.0000
$M_{ij,n}$; $i = j$	1.0000	0.0000	0.0000	0.0000	0.0000	0.0000	0.0000	0.0000
$K_{11,n}$	1.7178	−0.6817	0.0843	−0.0803	0.0203	−0.0257	0.0067	−0.0090
$K_{22,n}$	1.2975	−0.2609	0.0163	−0.0287	0.0036	−0.0093	0.0012	−0.0034
$K_{33,n}$	1.1869	−0.1595	0.0066	−0.0173	0.0015	−0.0056	0.0005	−0.0020
other $K_{ij,n}$	0.0000	0.0000	0.0000	0.0000	0.0000	0.0000	0.0000	0.0000

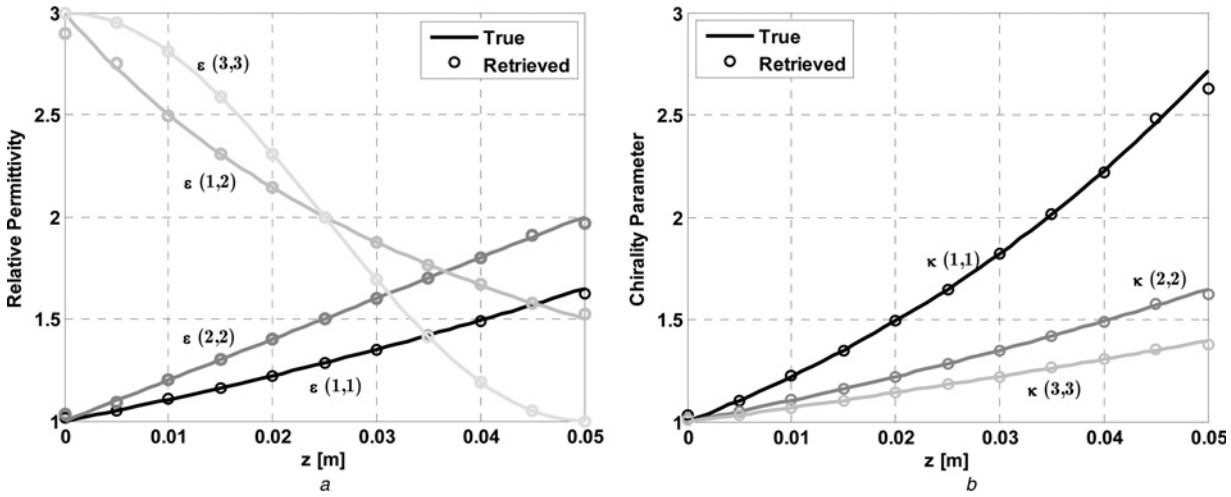

Fig. 3 *Comparison of the retrieved and true inhomogeneous bianisotropic slab in free space*

a Relative permittivity
b Chirality parameter

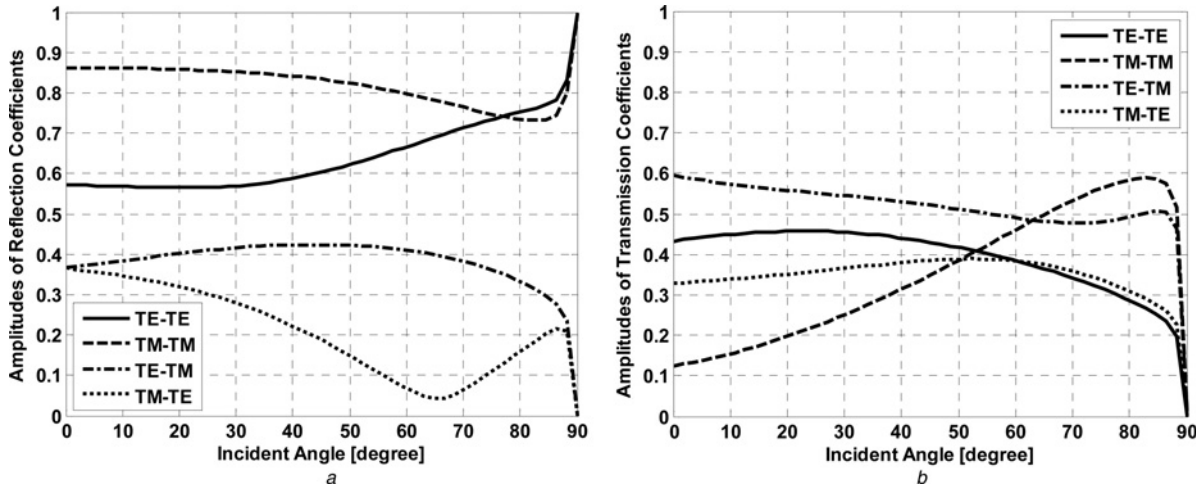

Fig. 4 *Amplitudes of co- and cross-reflection and transmission coefficients as a function of incident angle θ_i for inhomogeneous bianisotropic slab*

a Reflection slab discussed in example 2
b Transmission

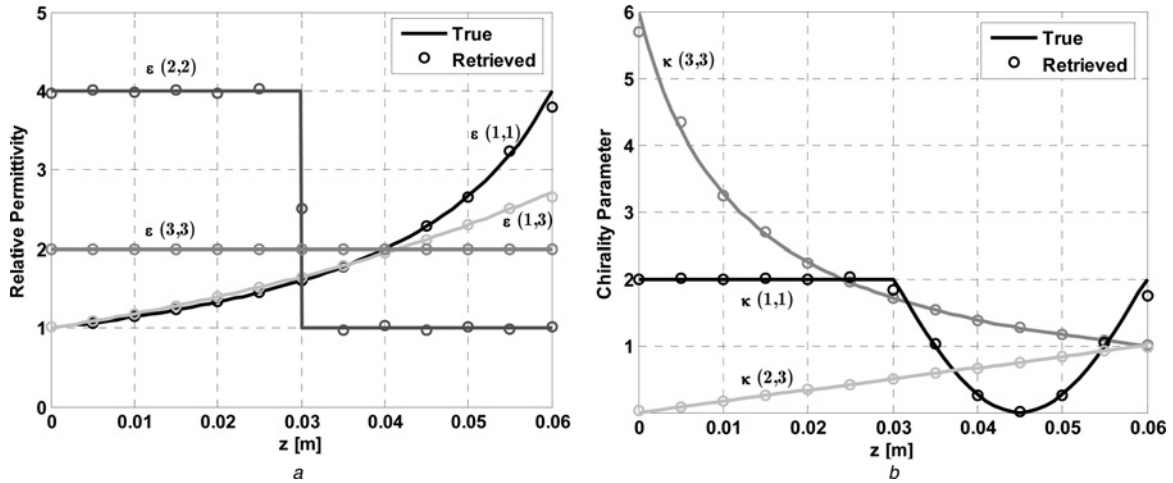

Fig. 5 *Comparison of the retrieved and true unknown functions of inhomogeneous bianisotropic slab in free space*

a Relative permittivity
b Chirality parameter

IET Microw. Antennas Propag., 2013, Vol. 7, Iss. 6, pp. 436–443
doi: 10.1049/iet-map.2012.0553

inhomogeneous chiral slab are known and the co- and cross-polarised reflection and transmission coefficients are generated using the notation of propagators method, that is, performing a forward procedure. Then, the electromagnetic parameters are assumed to be unknown and the reflection and transmission coefficients are used to calculate such parameters, that is, performing an inverse procedure. As the second example, a non-magnetic inhomogeneous bianisotropic slab is considered with thickness of $d = 6$ cm, and the more complex relative permittivity and chirality parameter tensors as

$$\bar{\bar{\varepsilon}}(z) = \varepsilon_0 \begin{pmatrix} \dfrac{4}{4-3(z/d)} & 0 & \exp\left(\dfrac{z}{d}\right) \\ 0 & \begin{cases} 4 & 0 \le z \le 0.5d \\ 1 & 0.5d \le z \le d \end{cases} & 0 \\ \exp\left(\dfrac{z}{d}\right) & 0 & 2 \end{pmatrix} \tag{14}$$

$$\bar{\bar{\kappa}}(z) = \begin{pmatrix} \begin{cases} 2 & 0 \le z \le 0.5d \\ 2+2\sin\left(\dfrac{2\pi z}{d}\right) & 0.5d \le z \le d \end{cases} & 0 & 0 \\ 0 & 1 & \left(\dfrac{z}{d}\right) \\ 0 & \left(\dfrac{z}{d}\right) & \dfrac{6}{1+5(z/d)} \end{pmatrix} \tag{15}$$

The amplitudes of co- and cross-reflection and transmission coefficients against the angle of incidence at excitation frequency of 1 GHz obtained from the forward problem solver are shown in Fig. 4. Assuming $N = 11$ in (7–9), calculation of the unknown coefficients of Fourier expansions of constitutive parameters is done through the utilisation of GSA that minimises the error between the measured and calculated data. The results of this reconstruction algorithm are given in Table 2. The final retrieved unknown functions are compared with the true ones in Figs. 5*a* and *b*. The profiles generated by the proposed technique and the corresponding exact values are in very good agreement, which indicates that the retrieval method is feasible and robust.

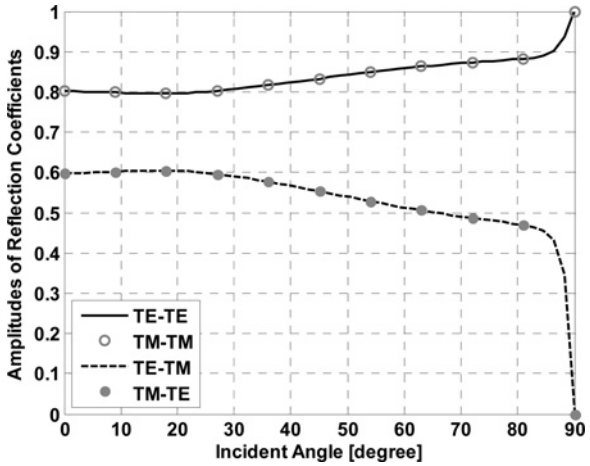

Fig. 6 *Amplitudes of co- and cross-reflection coefficients as a function of incident angle θ_i for PEC backed inhomogeneous bianisotropic slab*

Table 2 Optimisation results for the truncated Fourier series expansions of electromagnetic parameters of PEC backed inhomogeneous bianisotropic slab (example 2)

Coefficients	$n=0$	$n=1$	$n=2$	$n=3$	$n=4$	$n=5$	$n=6$	$n=7$	$n=8$	$n=9$	$n=10$	$n=11$
$E_{11,n}$	1.8454	−0.9861	0.3198	−0.2061	0.1067	−0.0820	0.0485	−0.0399	0.0241	−0.0198	0.0103	−0.0069
$E_{13,n}$	1.7176	−0.6826	0.0836	−0.0811	0.0202	−0.0281	0.0082	−0.0131	0.0038	−0.0065	0.0014	−0.0027
$E_{22,n}$	2.4995	1.8976	−0.0009	−0.6028	−0.0010	0.3243	−0.0008	−0.1998	−0.0008	0.1172	−0.0007	−0.0564
$E_{33,n}$	2.0000	0.0000	0.0000	0.0000	0.0000	0.0000	0.0000	0.0000	0.0000	0.0000	0.0000	0.0000
other $E_{ij,n}$	0.0000	0.0000	0.0000	0.0000	0.0000	0.0000	0.0000	0.0000	0.0000	0.0000	0.0000	0.0000
$M_{ij,n}$, $i = j$	1.0000	0.0000	0.0000	0.0000	0.0000	0.0000	0.0000	0.0000	0.0000	0.0000	0.0000	0.0000
$K_{11,n}$	1.3534	0.8608	−0.0051	−0.4972	0.4047	−0.1084	−0.0064	−0.0429	0.0608	−0.0184	−0.0033	−0.051
$K_{22,n}$	1.000	0.0000	0.0000	0.0000	0.0000	0.0000	0.0000	0.0000	0.0000	0.0000	0.0000	0.0000
$K_{23,n} = K_{32,n}$	0.5001	−0.4044	0.0001	−0.0441	0.0001	−0.0152	0.0001	−0.0073	0.0001	−0.0038	0.0001	−0.0017
$K_{33,n}$	2.1416	1.4338	0.5788	0.3784	0.2226	0.1669	0.1099	0.0857	0.0563	0.0427	0.0247	0.0144
other $K_{ij,n}$	0.0000	0.0000	0.0000	0.0000	0.0000	0.0000	0.0000	0.0000	0.0000	0.0000	0.0000	0.0000

Table 3 Optimisation results for the truncated Fourier series expansions of electromagnetic parameters of PEC backed inhomogeneous bianisotropic slab (example 3)

Coefficients	$n=0$	$n=1$	$n=2$	$n=3$	$n=4$	$n=5$	$n=6$	$n=7$
$E_{11,n}$	2.5000	−0.4044	0.0000	−0.0433	0.0000	−0.0138	0.0000	−0.0047
$E_{13,n}$	3.0000	0.0000	0.0000	0.0000	0.0000	0.0000	0.0000	0.0000
$E_{22,n}$	1.7178	−0.6817	0.0843	−0.0803	0.0203	−0.0257	0.0067	−0.0090
$E_{33,n}$	0.8679	−0.6243	−0.0673	−0.0626	−0.0143	−0.0200	−0.0044	−0.0069
other $E_{ij,n}$	0.0000	0.0000	0.0000	0.0000	0.0000	0.0000	0.0000	0.0000
$M_{ij,n}$; $i=j$	1.0000	0.0000	0.0000	0.0000	0.0000	0.0000	0.0000	0.0000
$K_{11,n}$	1.7178	−0.6817	0.0843	−0.0803	0.0203	−0.0257	0.0067	−0.0090
$K_{22,n}$	0.5000	0.0000	0.0000	0.0000	0.0000	0.0000	0.0000	0.0000
$K_{23,n}=K_{32,n}$	0.5000	−0.4044	0.0000	−0.0433	0.0000	−0.0138	0.0000	−0.0047
$K_{33,n}$	1.2975	−0.2609	0.0163	−0.0286	0.00358	−0.0093	0.0012	−0.0034
other $K_{ij,n}$	0.0000	0.0000	0.0000	0.0000	0.0000	0.0000	0.0000	0.0000

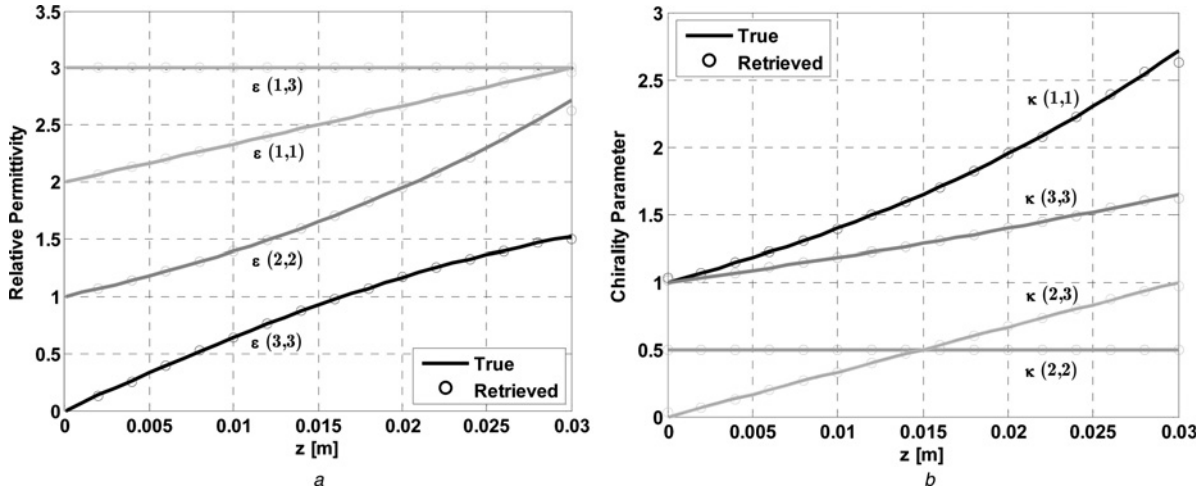

Fig. 7 *Comparison of the retrieved and true unknown functions of PEC backed inhomogeneous bianisotropic slab*

a Relative permittivity
b Chirality parameter

4.3 Example 3

In the third example, a PEC backed inhomogeneous bianisotropic slab with thickness of $d=3$ cm is considered. Typical profiles of the relative permittivity and chirality parameter tensors used for this non-magnetic slab are

$$\bar{\bar{\varepsilon}}(z)=\varepsilon_0\begin{pmatrix} 2+\frac{z}{d} & 0 & 3 \\ 0 & \exp\left(\frac{z}{d}\right) & 0 \\ 3 & 0 & 2\tanh\left(\frac{z}{d}\right) \end{pmatrix} \tag{16}$$

$$\bar{\bar{\kappa}}(z)=\begin{pmatrix} \exp\left(\frac{z}{d}\right) & 0 & 0 \\ 0 & 0.5 & \left(\frac{z}{d}\right) \\ 0 & \left(\frac{z}{d}\right) & \exp\left(\frac{z}{2d}\right) \end{pmatrix} \tag{17}$$

In this case, because of the PEC boundary condition at $z=d$, the co- and cross-transmission coefficients of the inhomogeneous slab at $z=0$ are zero. Therefore the objective function should be defined as

$$F=\sum_{\text{TE,TM}}\sum_{\theta=0}^{\pi/2}\left[\left|\tilde{R}_{\text{co}}(\theta)-R^m_{\text{co}}(\theta)\right|+\left|\tilde{R}_{\text{cross}}(\theta)-R^m_{\text{cross}}(\theta)\right|\right] \tag{18}$$

The amplitudes of co- and cross-reflection coefficients against the angle of incidence at frequency 1 GHz are shown in Fig. 6. Assuming $N=7$ in (7–9), calculation of the unknown coefficients of Fourier expansions of constitutive parameters is done through the utilisation of GSA that minimises the error between the measured and calculated data. The results of this reconstruction algorithm are given in Table 3. The final retrieved unknown functions are compared with the true ones in Figs. 7*a* and *b*. The results show that the accuracy of the inversion is quite satisfactory and all of the constitutive parameters are retrieved successfully indicating that the retrieval method is feasible and robust.

It is evident that, as the number of unknown coefficients in Fourier series expansions increases the accuracy of the solution increases. Also, as the thickness of the slab with respect to the wavelength increases, the necessary number of unknown coefficients increases.

doi: 10.1049/iet-map.2012.0553

5 Conclusions

An inversion algorithm is proposed to reconstruct the constitutive parameters profiles of an inhomogeneous bianisotropic slab using the co- and cross-reflection and transmission coefficients. In the proposed method, the permittivity, permeability and chirality parameter tensors of inhomogeneous bianisotropic layer are expanded using truncated Fourier series expansions. Then the unknown coefficients of these series are optimised through advanced and robust GSA method so that the calculated co- and cross-reflection and transmission data match the measured ones. The use of GSA optimisation method is extremely effective in saving a lot of computation time during the inversion process. In order to investigate the applicability of the proposed inversion method, three different inversion problems including an inhomogeneous bianisotropic layer in free space and a PEC backed one are considered and analysed. The results indicate that the constitutive parameters tensors of the inhomogeneous bianisotropic slabs are retrieved successfully, and the method is feasible and robust.

6 References

1 Serdyukov, A., Semchenko, I., Tretyakov, S.A., Sihvola, A.: 'Electromagnetics of bi-anisotropic materials: theory and applications' (Gordon and Breach Science Publishers, 2001)

2 Tretyakov, S.A., Sochava, A.A.: 'Proposed composite material for nonreflecting shields and antenna radomes', *IET Electron. Lett*., 1993, **29**, (12), pp. 1048

3 Yang, R., Xie, Y., Li, X.: 'Slow wave propagation in nonradiative dielectric waveguides with bianisotropic split ring resonator metamaterials', *Infrared Phys. Technol*., 2008, **51**, (6), pp. 555–558

4 Butylkin, V., Kraftmakher, G.: 'Passbands of bianisotropic and waveguide bianisotropic metamaterials based on planar double split rings', *J. Commun. Technol. Electron*., 2008, **53**, (1), pp. 1–14

5 Prosvirnin, S.L., Zheludev, N.I.: 'Analysis of polarization transformations by a planar chiral array of complex-shaped particles', *J. Opt. A, Pure Appl. Opt*., 2009, **11**, (7), pp. 074002

6 Pelet, P., Engheta, N.: 'Novel rotational characteristics of radiation patterns of chirostrip dipole antennas', *Microw. Opt. Technol. Lett*., 1992, **5**, (1), pp. 31–34

7 Chemseddine, Z., Fatiha, B.: 'Asymptotic approach for rectangular microstrip patch antenna with magnetic anisotropy and chiral substrate', *Int. J. Electron., Circuits Syst*., 2009, **3**, (2), pp. 84–90

8 Landy, N., Bingham, C., Tyler, T.: 'Design, theory, and measurement of a polarization-insensitive absorber for terahertz imaging', *Phys. Rev. B*, 2009, **79**, (12), pp. 125104

9 Tretyakov, S.A., Simovski, C.R., Hudlicka, M.: 'Bianisotropic route to the realization and matching of backward-wave metamaterial slabs', *Phys. Rev. B*, 2007, **75**, (15), pp. 153104

10 Guven, K., Saenz, E., Gonzalo, R.: 'Electromagnetic cloaking with canonical spiral inclusions', *New J. Phys*., 2008, **10**, (11), pp. 115037

11 Demir, V., Elsherbeni, A.Z., Arvas, E.: 'FDTD formulation for dispersive chiral media using the Z transform method', *IEEE Trans. Antennas Propag*., 2005, **53**, (10), pp. 3374–3384

12 Nayyeri, V., Soleimani, M., Rashed-Mohassel, J., Dehmollaian, M.: 'FDTD modeling of dispersive bianisotropic media using Z-transform method', *IEEE Trans. Antennas Propag*., 2011, **59**, (6), pp. 2268–2279

13 Valor, L., Zapata, J.: 'An efficient finite element formulation to analyze waveguides with lossy inhomogeneous bi-anisotropic materials', *IEEE Trans. Microw. Theory Tech*., 1996, **44**, pp. 291–296

14 Rikte, S., Kristensson, G., Anderson, M.: 'Propagation in bianisotropic media-reflection and transmission', *IEEE Proc. Microw. Antennas Propag*., 2001, **148**, (1), pp. 29–36

15 Richmond, J.H.: 'Transmission through inhomogeneous plane layers', *IRE Trans. Antennas Propag*., 1962, pp. 300–305

16 Chew, W.C.: 'Waves and fields in inhomogeneous media' (IEEE Press, 1990)

17 Urbani, F., Vegni, L., Toscano, A.: 'Inhomogeneous layered planar structures: an analysis of the reflection coefficients', *IEEE Trans. Magn*., 1998, **34**, (5), pp. 2771–2774

18 Vegni, L., Toscano, A.: 'Full-wave analysis of planar stratified with inhomogeneous layers', *IEEE Trans. Antennas Propag*., 2000, **48**, (4), pp. 631–633

19 Khalaj-Amirhosseini, M.: 'Analysis of lossy inhomogeneous planar layers using Taylor's series expansion', *IEEE Trans. Antennas Propag*., 2006, **54**, (1), pp. 130–135

20 Khalaj-Amirhosseini, M.: 'Analysis of lossy inhomogeneous planar layers using Fourier series expansion', *IEEE Trans. Antennas Propag.*, 2007, **55**, (2), pp. 489–493

21 Khalaj-Amirhosseini, M.: 'An approximated closed-form solution for inhomogeneous planar layers', *IET Microw. Antennas Propag*., 2007, **13**, (6), pp. 899–905

22 Zarifi, D., Abdolali, A., Soleimani, M., Nayyeri, V.: 'Inhomogeneous planar layered chiral media: analysis of wave propagation and scattering using Taylor's series expansion', *Prog. Electromagn. Res*., 2012, **125**, pp. 119–135

23 Nayyeri, V., Zarifi, D., Soleimani, M.: 'Electromagnetic scattering from inhomogeneous planar layered media using notation of propagators', *J. Electromagn. Waves Appl*., 2012, **26**, (6), pp. 875–884

24 Chen, X., Grzegorczyk, T.M., Kong, JA.: 'Optimization approach to the retrieval of the constitutive parameters of slab of general bianisotropic medium', *Prog. Electromagn. Res*., 2006, **60**, pp. 1–18

25 Avriel, M.: 'Non linear programming: analysis and methods' (Dover Publications, 2003)

26 Abubakar, A., Habashy, T.M., Druskin, V.L., Knizhnerman, L.: 'An enhanced Gauss-Newton inversion algorithm using a dual-optimal grid approach', *IEEE Trans. Geosci. Remote Sens*., 2006, **44**, pp. 1419–1427

27 Caorsi, S., Costa, A., Pastorino, M.: 'Microwave imaging within the second-order Born approximation: Stochastic optimization by a genetic algorithm', *IEEE Trans. Antennas Propag*., 2001, **49**, (1), pp. 22–31

28 Donelli, M., Franceschini, D., Rocca, P., Massa, A.: 'Three dimensional microwave imaging problems solved through an efficient multiscaling particle swarm optimization', *IEEE Trans. Geosci. Remote Sens.*, 2009, **47**, pp. 1467–1481

29 Rashedi, E., Nezamabadi-pour, H., Saryazdi, S.: 'GSA: a gravitational aearch algorithm', *Inf. Sci*., 2009, **179**, pp. 2232–2248